


RESEARCH ARTICLE

Synthesis of colorless polyimides derived from benzimidazole diamines with bis-amide structures

Hao Zhang¹ | Feng Guo¹ | Ke Xu¹ | Mengxia Wang¹ | Chunhai Chen¹ |
Guangtao Qian² | Gang Liu¹  | Zhiqing Deng³

¹State Key Laboratory for Modification of Chemical Fibers and Polymer Materials, Center for Advanced Low-dimension Materials, College of Material Science and Engineering, Donghua University, Shanghai, People's Republic of China

²Center for Civil Aviation Composites, Donghua University, Shanghai, People's Republic of China

³Shanghai Institute of Precision Measurement and Test, Shanghai, China

Correspondence

Guangtao Qian, Center for Civil Aviation Composites, Donghua University, Shanghai, People's Republic of China.
Email: qgt@dhu.edu.cn

Gang Liu, State Key Laboratory for Modification of Chemical Fibers and Polymer Materials, Center for Advanced Low-dimension Materials, College of Material Science and Engineering, Donghua University, Shanghai, People's Republic of China.
Email: liugang@dhu.edu.cn

Funding information

Fundamental Research Funds for the Central Universities, Grant/Award Number: 2232023D-23

Abstract

To make the colorless polyimides (CPIs) suitable for the application of flexible display technology, the polyimide (PI) films need to have both good optical properties and thermal properties. To get the wanted properties, 2-(2-methyl-4-(2-methyl-4-aminobenzamido)phenyl)-5-(2-methyl-4-aminobenzamido)-*N*-phenylbenzimidazol (5a) and 2-(2-methyl-4-(2-trifluoromethyl-4-aminobenzamido)phenyl)-5-(2-trifluoromethyl-4-aminobenzamido)-*N*-phenylbenzimidazol (5b) were synthesized, which both contained benzimidazole and bis-amide structures. Two kinds of PI films were polymerized with cyclobutane-1,2,3,4-tetracarboxylic dianhydride (CBDA). With the contribution of side groups ($-\text{CH}_3$ or $-\text{CF}_3$), the resulting PI films presented relatively superior optical properties (transmittance at 400 nm was 59% and 68% respectively) and low coefficient of thermal expansion ($\text{CTE} = 22$ and 25 ppm K^{-1}). These good properties suggest that these PI films have the potential for flexible display usage.

KEYWORDS

colorless polyimide, benzimidazole, bis-amide structure, dimensional stability

1 | INTRODUCTION

With the development of flexible display technology, various techniques have been developed to synthesize polymer films to take the place of traditional glass. Polyimides (PIs) obtain extensive research due to their excellent comprehensive properties, such as flexibility, lightweight, outstanding thermal and mechanical properties, and environmental stabilities.¹ Therefore, they are potential substitutes for light-emitting diodes and flexible optoelectronic devices (OLEDs).^{2–6} To

manufacture the display devices, in addition to having good optical properties, the PIs need to withstand thin-film transistor formation ($T_g > 300^\circ\text{C}$) and keep a low coefficient of thermal expansion ($\text{CTE} < 20 \text{ ppm K}^{-1}$).⁷ However, the charge transfer complex (CTC) effect derived from the diamine electron donor and dianhydride electron acceptor of the backbone of PI makes the molecular chains pack tightly to become a highly conjugated structure. This is the reason for strong absorption in the visible light and near-infrared range, which also leads to a darker color.^{8,9}

To make the PIs colorless, massive research has been done and several methods were given, such as introducing fluorinated segments, alicyclic units, bulky substituents, and rigid but non-coplanar moieties.^{10–15} Introducing these groups can effectively enlarge the inter-chain distance, so the degree of molecular aggregation can be lower.¹⁶ However, these methods will weaken the thermal properties such as higher CTE, making the CTE between PIs and their contact material incompatible, which will cause thermal stress and reduce the reliability of the devices eventually. To balance the optical transmittance and thermal dimensional stability, a certain proportion of rigid structural units should be added as well.¹⁷ To achieve a low CTE, much research has been done to increase the rigidity of the main chain or strengthen the inter-chain interactions, such as adding inorganic nanoparticles filler with low CTE, in situ polymerization to build hydrogen-bond network, and designing of more rigid/linear molecular structure.^{18–21} In various rigid structures, the amide and benzanilide linkage and cyclobutane-1,2,3,4-tetracarboxylic dianhydride(CBDA) are commonly used.^{22–24}

Based on our previous study, 6-amino-2-(2'-methyl-4'-aminobenzene)-*N*-phenylbenzimidazol was continued to use to make sure that the PIs had good chemical heat resistance.^{25,26} Two novel benzimidazole diamines, 2-(2-methyl-4-(2-methyl-4-aminobenzamido)phenyl)-5-(2-methyl-4-aminobenzamido)-*N*-phenylbenzimidazol (5a) and 2-(2-methyl-4-(2-trifluoromethyl-4-aminobenzamido)phenyl)-5-(2-trifluoromethyl-4-aminobenzamido)-*N*-phenylbenzimidazol (5b) were synthesized. The bis-amide was introduced to ensure the stiff/linear structure to control the dimensional change.²⁷ The methyl ($-\text{CH}_3$) or trifluoromethyl ($-\text{CF}_3$) were introduced to optimize the optical properties.²⁸ The crank-shaft-like steric structure of CBDA was good for in-plane orientation, maintaining structural rigidity, linearity, and high heat resistance.^{29–31} Finally, two kinds of colorless PIs were prepared and the properties data showed the possibility for further use.

2 | EXPERIMENTAL

2.1 | Materials

6-Amino-2-(2'-methyl-4'-aminobenzene)-*N*-phenylbenzimidazol (MPBZ) was synthesized by previously reported methods.²⁵ Triethylamine (Et_3N), palladium 10% on charcoal (Pd/C), 85% hydrazine monohydrate ($\text{N}_2\text{H}_4\cdot\text{H}_2\text{O}$) and isoquinoline were obtained from Sinopharm Chemical Reagent Shanghai Co., Ltd. Tetrahydrofuran (THF), *m*-cresol, *N,N*-dimethylacetamide (DMAc), thionyl chloride(SOCl_2) and other solvents were purchased from

Shanghai Aladdin Biochemical Technology Co., Ltd. and used as received. 2-Methyl-4-nitrobenzoic acid and 4-nitro-2-(trifluoromethyl)benzoic acid was purchased from Shanghai Titan Scientific Co., Ltd. 1,2,3,4-Cyclobutanetetracarboxylic dianhydride was supplied by Tokyo Chemical Industry (Shanghai), which were dried in a vacuum oven at 80 °C before used.

2.2 | Measurements

The Nuclear magnetic resonance (NMR) spectra were obtained by Bruker 400 AVANCE III spectrometer with deuterated solvent (Dimethyl sulfoxide- d_6). Elementar Vario EL-III was used to analyze the elemental composition of monomers. Fourier transform infrared (FTIR) spectra were obtained on Nicolet 6700 FTIR spectrometer with attenuated total reflectance (ATR) mode. To get the wide-angle X-ray diffraction (WXR) a Rigaku Denki D/MAX-2500 diffractometer with Cu $K\alpha$ radiation ($\lambda = 1.54 \text{ \AA}$) was used. With DMF as the eluent and polystyrene as an external standard, the Waters GPC Systems was used to get the information about weight-average (M_w) and number-average (M_n) molecular weights. Assessed by Hangzhou color spectrum CS-720 colorimeter with an observational angle of 10°, the color intensities were measured. The transmittance of the films was measured by a Shimadzu UV-3600 spectrophotometer in the wavelength range of 200–800 nm. Dynamic mechanical analysis (DMA) was assessed by using RSA-G2 in a tension mode with a heating rate of 5 °C min^{-1} . From 40 °C to 350 °C, with a constant heating rate of 5 °C min^{-1} and a fixed load of 0.5 g μm^{-1} (film thickness), the CTE was investigated by TMA Q400. Discovery TGA 550 was used with a constant heating rate of 10 °C min^{-1} under a nitrogen atmosphere to get the thermogravimetric analysis (TGA) information ranging from 40 °C to 800 °C. Average mechanical properties were tested by Instron 5966 universal testing machine with the testing speed of 5 mm min^{-1} and the samples were made into a size of 5 mm in width and 50 mm in length, the initial moduli are calculated by the method of interval of initial slope. The solubility was investigated by adding 10 mg of the PI powder in 1 mL of chosen solvents at room temperature for 24 h. The Water absorption (W_A) of the films was determined by the weight change between dry films and wet films. The samples were made into dimensions of 50 × 50 mm and were dried in a vacuum oven at 80 °C for 24 h and weighed. After being drowned in water at 25 °C for 24 h, the samples were wiped clean and weighed again. The water absorption was determined by Equation (1):

$$W_A = \frac{(m_1 - m_0)}{m_0} \times 100\% \quad (1)$$

where m_0 and m_1 represented the sample's dry mass and wet mass, respectively. Each W_A was averaged over three parallel samples.

2.3 | Synthesis of diamines

2.3.1 | 2-(2-Methyl-4-(2-methyl-4-nitrobenzamido)phenyl)-5-(2-methyl-4-nitrobenzamido)-*N*-phenylbenzimidazol(4a)

First, 2-methyl-4-nitrobenzoic acid (10.00 g, 55.2 mmol) was added into a 250 mL round-bottom flask with thionyl chloride (70 mL) as solvent reflux for 12 h then washed by THF. Second, THF (100 mL) was used to dissolve MPBZ (3.30 g, 10.5 mmol) in a 500 mL three-neck bottle and Et_3N (3.20 g, 31.6 mmol) was added. Thirty minutes later, the solution of the first step was added into the bottle under stirring. The reaction continued for 12 h under room temperature. The TLC was used to decide the extent of the reaction. The mixture was poured into water (200 mL) until the reaction was fully complete. Then, ethanol was used to filtrate and wash the product. Finally, the compound was moved into the vacuum oven at 100 °C for 24 h to get dried, and 5.27 g of a nitro compound (4a, yield: 78.3%) was obtained. ^1H NMR (400 MHz, $\text{DMSO}-d_6$, ppm): δ = 10.64 (s, 2H), 8.26–8.24 (m, 2H), 8.23 (d, J = 2.4 Hz, 1H), 8.17 (ddd, J = 10.3, 8.2, 2.4 Hz, 2H), 7.77 (dd, J = 16.4, 8.4 Hz, 2H), 7.68 (d, J = 2.1 Hz, 1H), 7.61 (dd, J = 8.8, 2.0 Hz, 1H), 7.52 (tt, J = 7.9, 1.4 Hz, 3H), 7.48–7.41 (m, 1H), 7.39–7.34 (m, 2H), 7.30 (dd, J = 8.6, 7.0 Hz, 2H), 2.55 (s, 5H), 2.54 (s, 3H), 2.21 (s, 3H). FTIR (ATR, ν , cm^{-1}): 3337 (NH in amide stretching), 1675, 1593 ($\text{C}=\text{N}/\text{C}=\text{C}$ stretching of ring), 1515, 1348 (NO_2 asymmetric and symmetric stretching), 1307 (imidazole ring breathing). Anal. Calcd for $\text{C}_{36}\text{H}_{28}\text{N}_6\text{O}_6$: C, 67.49; H, 4.41; N, 13.12. Found: C, 64.39; H, 4.73; N, 11.84.

2.3.2 | 2-(2-Methyl-4-(2-methyl-4-aminobenzamido)phenyl)-5-(2-methyl-4-aminobenzamido)-*N*-phenylbenzimidazol(5a)

4a (5.00 g, 7.80 mmol) and Pd/C (0.50 g) were added into a 250 mL round-bottom with ethanol (50 mL), and hydrazine hydrate (5.10 g, 159.13 mmol) was added dropwise. The reaction was carried out under 80 °C in a reflux situation for 6 h. The suspension was filtered and poured into 100 mL water. The

precipitate was collected by suction filtration and purified by recrystallization ($\text{DMSO}:\text{H}_2\text{O}$ = 2: 1) to obtain white powder 5a (4.20 g, yield: 92.7%). ^1H NMR (400 MHz, $\text{DMSO}-d_6$): δ = 9.92 (d, J = 2.1 Hz, 2H), 8.19 (d, J = 1.9 Hz, 1H), 7.65 (d, J = 2.1 Hz, 1H), 7.60 (dd, J = 8.8, 2.0 Hz, 1H), 7.52–7.45 (m, 3H), 7.44–7.38 (m, 1H), 7.34–7.27 (m, 3H), 7.26–7.16 (m, 4H), 6.43 (ddt, J = 8.4, 5.9, 2.5 Hz, 4H), 5.48 (s, 2H), 5.43 (s, 2H), 2.33 (s, 3H), 2.29 (s, 3H), 2.16 (s, 3H). FTIR (ATR, ν , cm^{-1}): 3230 (NH in amide stretching), 3571, 3424, 3346 (amine NH), 1645, 1599 ($\text{C}=\text{N}/\text{C}=\text{C}$ stretching of ring), 1249 (imidazole ring breathing). Anal. Calcd for $\text{C}_{36}\text{H}_{32}\text{N}_6\text{O}_2$: C, 74.46; H, 5.55; N, 14.47. Found: C, 72.13; H, 5.67; N, 13.98.

2.3.3 | 2-(2-Methyl-4-(2-trifluoromethyl-4-nitrobenzamido)phenyl)-5-(2-trifluoromethyl-4-nitrobenzamido)-*N*-phenylbenzimidazol(4b)

The 4b was prepared the same way as 4a. 5.15 g compound was obtained (yield: 65.6%). ^1H NMR (400 MHz, $\text{DMSO}-d_6$): δ = 10.88 (d, J = 4.9 Hz, 2H), 8.67–8.55 (m, 4H), 8.18 (d, J = 1.9 Hz, 1H), 8.08 (dd, J = 11.3, 8.4 Hz, 2H), 7.61 (d, J = 2.1 Hz, 1H), 7.57–7.48 (m, 3H), 7.48–7.41 (m, 2H), 7.39–7.28 (m, 4H), 2.21 (s, 3H). FTIR (ATR, ν , cm^{-1}): 3309 (NH in amide stretching), 1675, 1598 ($\text{C}=\text{N}/\text{C}=\text{C}$ stretching of ring), 1535, 1314 (NO_2 asymmetric and symmetric stretching), 1287 (imidazole ring breathing). Anal. Calcd for $\text{C}_{36}\text{H}_{22}\text{F}_6\text{N}_6\text{O}_6$: C, 57.76; H, 2.96; N, 11.23. Found: C, 56.91; H, 3.09; N, 10.96.

2.3.4 | 2-(2-Methyl-4-(2-trifluoromethyl-4-aminobenzamido)phenyl)-5-(2-trifluoromethyl-4-aminobenzamido)-*N*-phenylbenzimidazol(5b)

The 5b was prepared the same way as 5a and the 4.19 g compound was collected (yield: 91.1%). ^1H NMR (400 MHz, $\text{DMSO}-d_6$): δ = 10.28 (d, J = 6.1 Hz, 2H), 8.15 (d, J = 2.0 Hz, 1H), 7.62 (d, J = 2.1 Hz, 1H), 7.59–7.54 (m, 1H), 7.49 (dd, J = 8.2, 6.8 Hz, 2H), 7.45–7.39 (m, 3H), 7.37 (d, J = 6.0 Hz, 1H), 7.33 (dt, J = 8.1, 1.1 Hz, 3H), 7.23 (dd, J = 13.7, 8.6 Hz, 2H), 6.95 (dd, J = 6.1, 2.3 Hz, 2H), 6.85–6.77 (m, 2H), 5.93 (d, J = 15.3 Hz, 4H), 2.16 (s, 3H). FTIR (ATR, ν , cm^{-1}): 3226 (NH in amide stretching), 3487, 3443, 3363 (amine NH), 1613 ($\text{C}=\text{N}/\text{C}=\text{C}$ stretching of ring), 1266 (imidazole ring breathing). Anal. Calcd for $\text{C}_{36}\text{H}_{26}\text{F}_6\text{N}_6\text{O}_2$: C, 62.79; H, 3.81; N, 12.20. Found: C, 61.37; H, 3.98; N, 10.96.

2.4 | Synthesis of polymers

A one-step method was used to obtain these PIs, and the isoquinoline was used in cyclization. For example, at room temperature, 5a (5.8069 g, 10.0 mmol) and CBDA (1.9611, 10.0 mmol) were dissolved into *m*-cresol (23.3040 g) under an atmosphere of nitrogen. When the reactant was totally dissolved, isoquinoline (0.0258 g, 0.2 mmol) was added and the temperature was raised to 200 °C and kept stirring for 8 h. The solution was cooled and poured into ethanol (120 mL), and white fibrous PI was obtained. After several times of washing (ethanol) and redissolving (DMAc), the PI was moved into the vacuum to get dried. To obtain a PI film, the PI was redissolved in DMAc to prepare a 15 wt% liquid solution first. A 0.22 µm PTFE filter was used to remove insoluble content, and then the solution was tiled over a dust-free glass. The glass disc was put in an oven for 12 h under 160 °C. Then treat the disc under 300 °C for 10 min. Eventually, a PI film (~20 µm) was obtained. The film derived from 5a-CBDA was defined as PI1, while the film derived from 5b-CBDA was considered to be PI2. The film derived from MPBZ-CBDA was meant to be given as a comparison but it was extremely fragile.

3 | RESULTS AND DISCUSSION

3.1 | Molecular structure and characterization

With the amide group attached to the MPBZ's head and tail, respectively, two kinds of PIs were in a type of bis-amide structure (Scheme 1). Figure 1 shows the ¹H NMR spectra of dinitrointermediate (4a) and diamine (5a). The amide proton's characteristic signals were located at 10.64 ppm in dinitrointermediate while at 9.93 ppm in diamine. It was a symbol of success in the introduction of amide moieties. The amine proton at tide and tile were 5.49 and 5.44 ppm, indicating the dinitrointermediate had been reduced into diamine successfully. Figure 2 shows the ¹H NMR spectra of dinitrointermediate (4b) and diamine (5b). The amide proton's characteristic signals were located at 10.88 ppm in dinitrointermediate while at 10.28 ppm in diamine. The amide moieties were also introduced successfully. The dinitrointermediate was successfully reduced into diamine as the amine proton at tide and tile, which were 5.94 and 5.91 ppm. The chemical shifts of —NH₂ in 5b were stronger than 5a because the —CF₃ had a strong electron-withdrawing effect while the —CH₃ had an electron-donating effect, which also

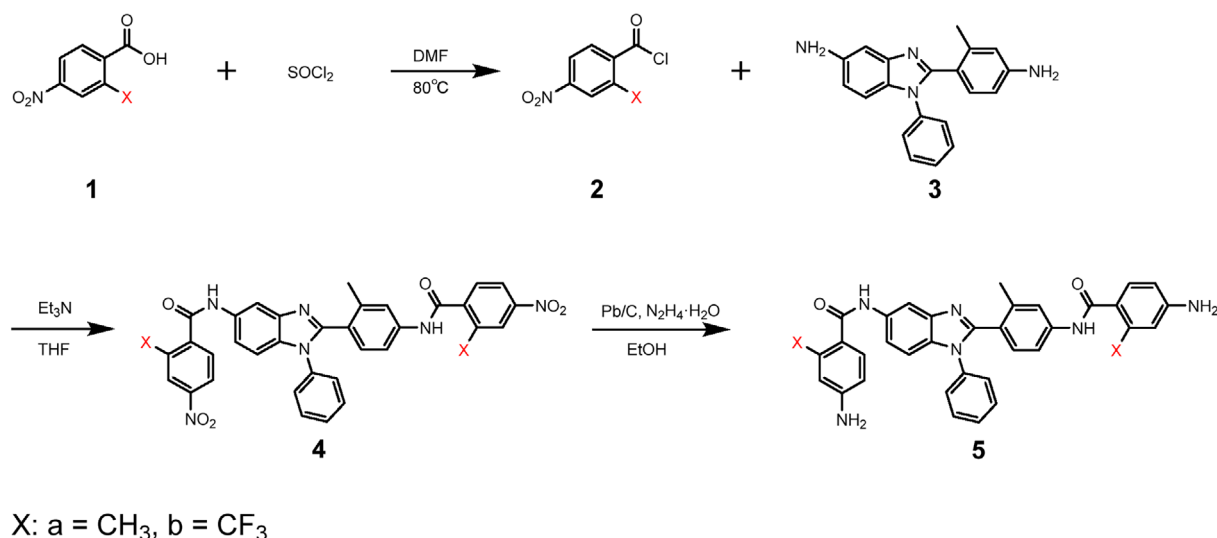
made 5a have higher nucleophilicity than 5b (Scheme 2).

3.2 | Polymer and molecular packing

As shown in Table 1, the number-average molecular weights (M_n) and weight-average molecular weights (M_w) of PI1 were 7.18×10^4 and 15.20×10^4 g mol⁻¹, respectively, and these values of PI2 were 1.95×10^4 and 2.90×10^4 g mol⁻¹ indicating the two polymer films had sufficient molecular weight. The order of number-average molecular weights were as follows PI1 > PI2, because the 5a in PI1 possessed higher nucleophilicity than 5b in PI2. The degree of polycondensation could be affected by the electron-donating property of terminal amino groups in the monomeric diamines, the higher electron-donating ability could strengthen the polycondensation to achieve higher molecular weights. This result could match the above-mentioned spectra of ¹H NMR.

Figure 3 was a summary of the obtained films' ATR-FTIR data. The amide and imidazole moiety structure of the PIs was confirmed by some characteristic bands. The peak at 3360 cm⁻¹ was attributed to the N—H stretching in —CONH—, and near 1662 cm⁻¹, it was amide C=O stretching. The imide C=O asymmetric stretching and symmetric stretching occurred at 1776 and 1708 cm⁻¹. The peak at 1369 cm⁻¹ belonged to imide C—N stretching and the imidazole breathing was at about 1306 cm⁻¹.^{32,33} The carbonyl absorption peak disappeared at 1660 cm⁻¹, indicating complete imidization of PI.^{25,34} However, the structure of —CONH— had an absorption of around 1662 cm⁻¹, which can be explained by the ¹H NMR spectrum (Figure 4). The peak of —COOH at 13.2 ppm was hardly observed, which was evidence of the high degree of imidization. The chemical shift at 3.82 ppm belonged to CBDA, which was another evidence to confirm the structural characteristics of the obtained PIs.

The further structural characteristics were investigated by Wide-Angle X-ray diffraction and presented in Figure 5. The PIs exhibited to be semi crystallization at a low level. The PI1 and PI2 exhibited peaks at $2\theta = 17.0^\circ$ and 14.3° , and the *d*-spacings were 5.211 and 6.189 Å (calculated by Bragg's law, $n\lambda = 2d \sin \theta$), which belonged to the amorphous part. The wide peaks at 17.0° and 14.3° confirmed the PIs were mostly amorphous. This result can be explained in two ways. First, the bulky *N*-phenyl pendant, —CH₃ or —CF₃ side groups had highly stereoscopic hindrance, which could disturb the self-chain alignment, resulting in loose



SCHEME 1 Reaction schemes for the synthesis of the biamide-containing benzimidazole diamines.

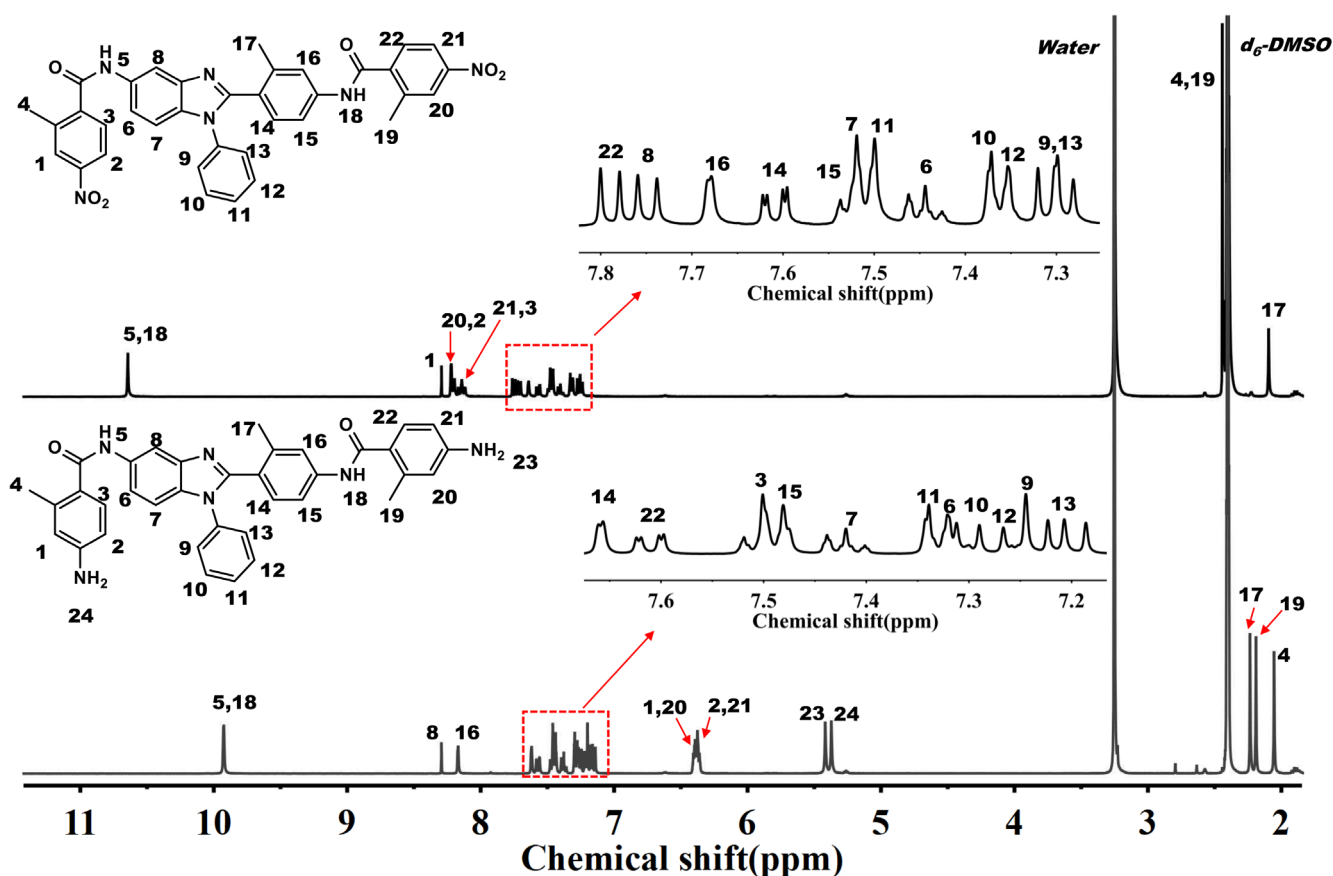


FIGURE 1 ¹H NMR spectra of 4a and 5a.

chain packaging and aggregation.^{31,35,36} Second, these substituent groups were in a twisted structure, which was also adverse to the chain packaging and

aggregation.³⁵ The *d*-spacing of PI1 was smaller than PI2, indicating the —CH₃ side group was smaller than —CF₃ and had less influence in chain packaging and

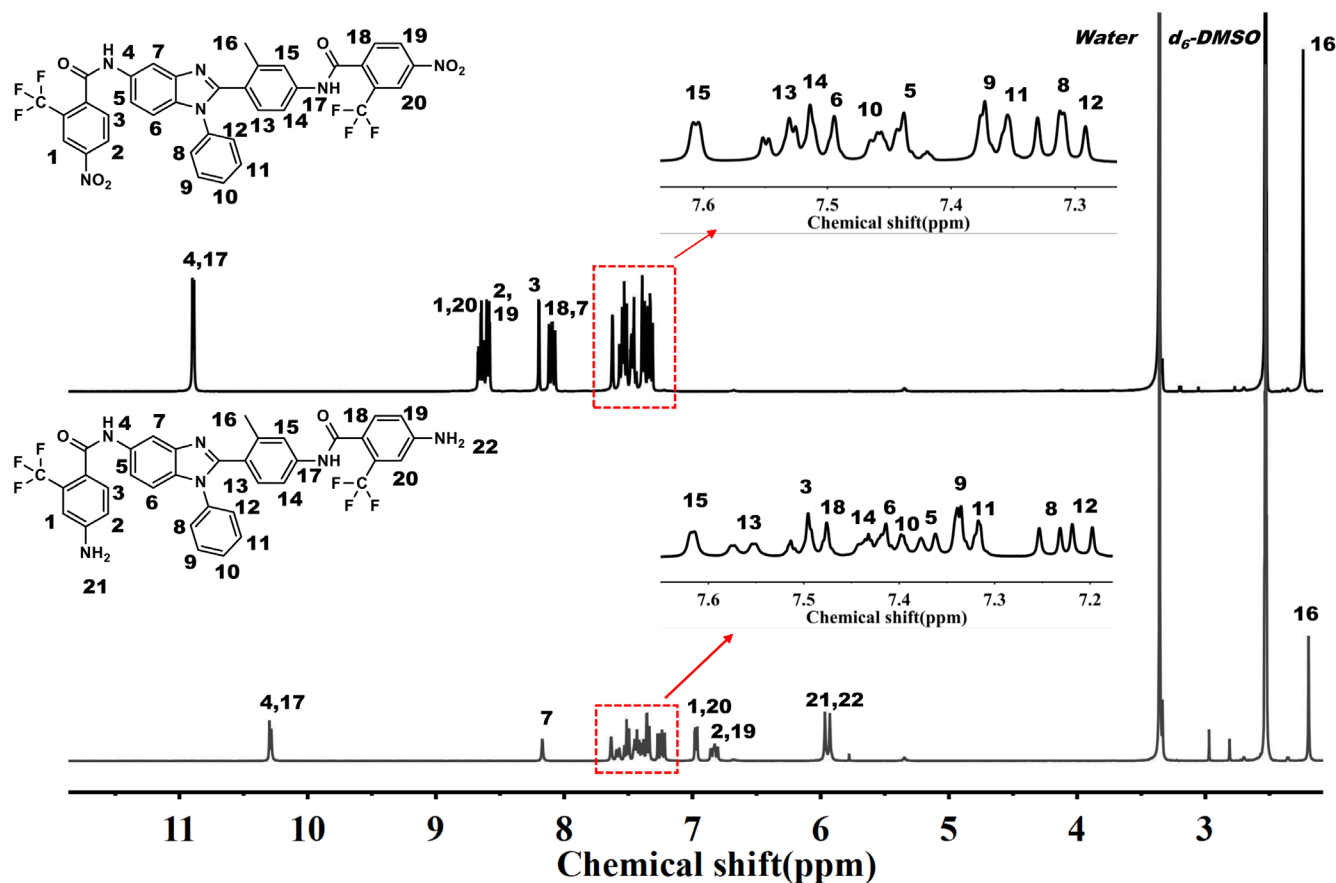
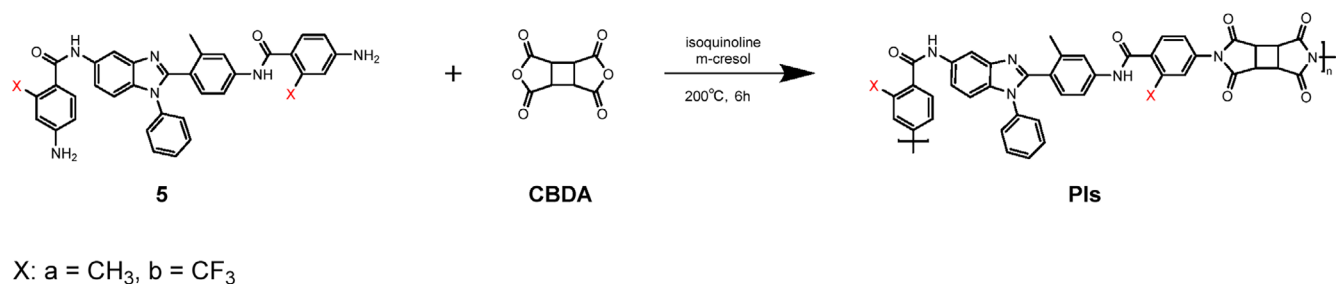


FIGURE 2 ^1H NMR spectra of 4b and 5b.



SCHEME 2 Synthetic routes to the semi-aromatic poly(benzimidazole imide)s.

TABLE 1 The molecular weights of the poly(benzimidazole imide)s.

PIs	Contents	$M_n (\times 10^4 \text{ g mol}^{-1})$	$M_w (\times 10^4 \text{ g mol}^{-1})$	PDI
PI1	5a-CBDA	7.18	15.20	2.12
PI2	5b-CBDA	1.95	2.90	1.49

aggregation. As for the crystallization zone, the $2\theta = 6.60^\circ$ and 6.56° , and the d -spacings were 13.38 and 13.46 Å. In this article, the temperature of imidization procedures was up to 300°C .^{37,38} And the high annealing temperature could make the structure of PIs more orderly.

3.3 | Solubility

Usually, it was insoluble for PIs in most organic solvents, so the terrible processing environment and preservation of intermediate (polyamide acid) could be a problem during the preparation process.^{39,40} To solve

those problems, the chemical imide preparation and one-step method were used, which required the PIs to become soluble. As the resulting PIs, CBDA could reduce the CTC effect, but the stiff structure made the inter-chain packing tighter, which was harmful to the solubility.³² However, the introduction of $-\text{CF}_3$ or $-\text{CH}_3$ side groups contributed to limiting the tight packing of molecular chains. The stacking density of

molecular chains was reduced so the diffusion and dissolution of molecular solvents were facilitated.³⁶ So as shown in Table 2, PI1 and PI2 could easily dissolve in commonly used high boiling solvents (NMP, DMAc, DMSO, DMF) without stirring or heating, which was better than our previous copolymer obtained by polymerization with HPMDA but without these side groups in diamines.³²

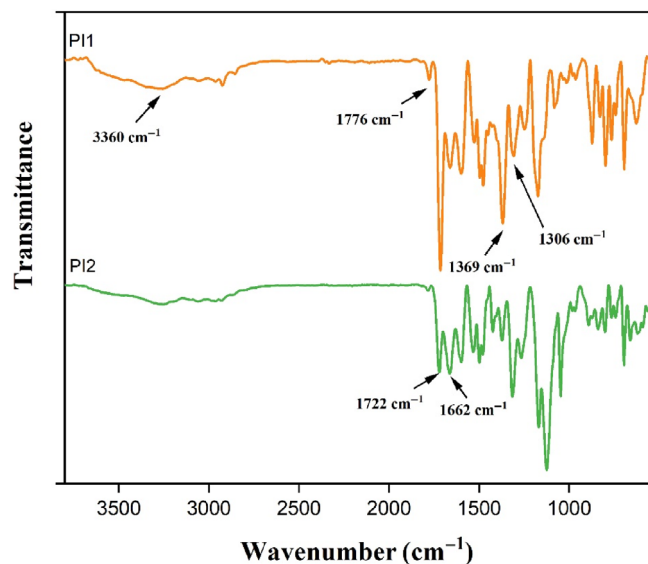


FIGURE 3 ATR-FTIR spectrum of poly(benzimidazole imide)s.

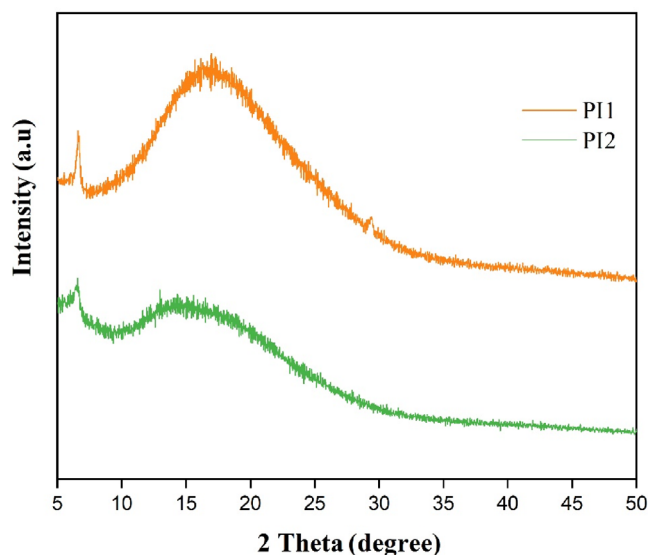


FIGURE 5 WAXD curves of the poly(benzimidazole imide) films.

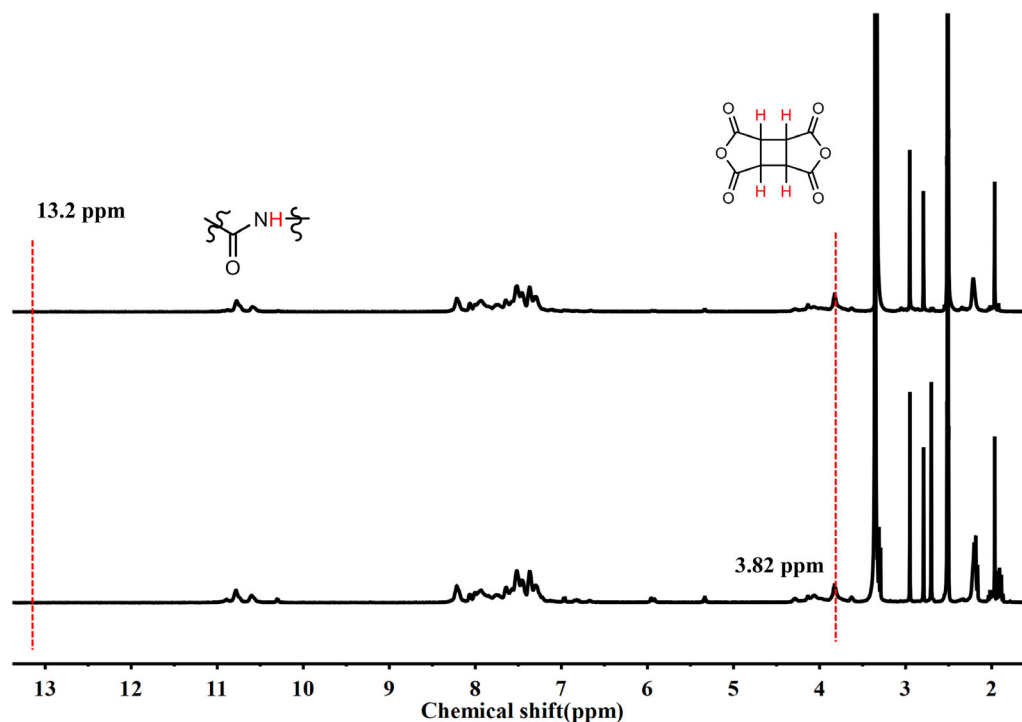
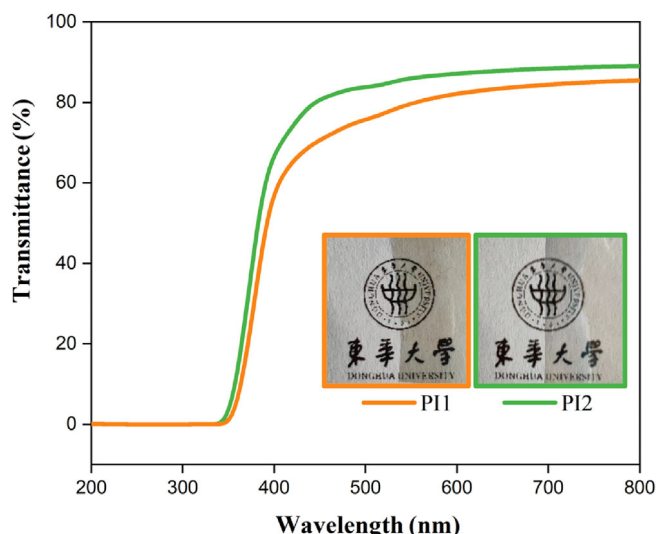


FIGURE 4 The ^1H NMR spectrum of poly(benzimidazole imide)s.

TABLE 2 Solubility of poly(benzimidazole imide) fibrous powders.

Solvents ^a	<i>m</i> -Cresol	NMP	DMAc	DMSO	DMF	THF	CHCl ₃
PIs							
PI1	±	+	+	+	+	—	—
PI2	±	+	+	+	+	—	—

[†]Soluble at room temperature; ±, partially soluble or swelling; —, insoluble.^aSolubility was determined with 10 mg of PIs in 1 mL of solvent at room temperature for 24 h.**FIGURE 6** UV-vis spectra and images of the poly(benzimidazole imide)s films.

3.4 | Optical properties

The monomers' structure and the polymer backbone stacking were two main effects on CTC, which could highly influence the color intensity of PI films. To control the CTC, an effective way was to decrease the inter-chain packing, such as introducing bulk side groups in monomers or using cycloaliphatic dianhydrides to take the place of aromatic dianhydrides.⁷ In this article, in order to control the CTC, —CH₃ or —CF₃ were introduced to loosen the packing density. The transmittance at 400 nm (T_{400}) is shown in Figure 6. T_{400} = 59% for PI1 and T_{400} = 68% for PI2 indicated that the electronegativity and steric torsion could reduce the CTC more effectively despite the stiff/liner structure of CBDA.¹⁰ As represented in Table 3, PI2 with —CF₃ side groups had higher lightness values (L^*), lower redness values (a^*), yellowness values (b^*), and yellowness index values (YI) than PI1 with —CH₃ side groups, due to the large steric hindrance and electronegativity of —CF₃ substituent.^{41,42}

3.5 | Thermal properties

Figure 7 and Table 4 show the glass-transition temperature (T_g) of PI films, which was determined by the peak temperature of the $\tan \theta$ curve with DMA. The T_g of PI1 and PI2 were 386 and 351 °C, respectively, indicating good heat-resistance properties suitable for the soldering process ($T_g > 300$ °C). One of the reasons for high T_g was contributed by the *N*-phenylbenzimidazol. The backbone rotational freedom of the PIs could be reduced by *N*-phenyl for its rigid pendant group.⁴³ The other reason was believed to be the strong dipole-dipole interaction of the imide carbonyl unities. However, the —CH₃ or —CF₃ effectively enlarged the inter-chain distance. The degree of molecular aggregation had been weakened, which was harmful to the thermal properties.¹⁶ So the T_g of PI1 and PI2 were lower than our previous work without these side groups.³²

To make sure the OLED devices run well, dimensional stability was essential. The dimensional stability of the films was determined by the average CTE values in the range of 100–300 °C (Figure 8). Research showed that CTE was affected by the in-plane orientation with chain stiffness/linearity and polymer backbones intermolecular interaction. In this work, the amide with crank-shaft-like groups was introduced, which strengthened the rigidity of the backbone by its liner structure and physical interaction by forming more hydrogen bonds between adjacent molecular chains. There were two kinds of hydrogen bonds. One was between the C=O in imide rings and N—H of the amide group. The other was the interaction between two amide groups.⁴⁴ The structure of CBDA was relatively liner steric in an anti-form and its cyclobutene ring could inhibit the rotational motions.^{29,45} Although the —CH₃ or —CF₃ side groups could widen the free space volume to weaken the in-plane orientation, the CTE of PI1 and PI2 could still reach 22 and 25 ppm K^{−1} respectively with the contribution of amide groups and CBDA.

To describe the chemical heat resistance, the thermal decomposition temperatures for 5% weight loss

PIs ^a	<i>d</i> (μm)	<i>a</i> *	<i>b</i> *	<i>L</i> *	YI	λ_{cutoff} (nm)	<i>T</i> ₄₀₀ (%)
PI1	24	0.03	3.95	94.44	7.96	355	59
PI2	20	−0.05	2	95.59	4.13	361	68

^a*d* was film thickness. Red color was meant by a positive *a**, while a negative *a** indicated green color. A positive *b** meant yellow color and a negative *b** indicated blue color. Lightness was determined by *L**: 100 meant white, while 0 indicated black. YI meant the yellowness index. λ_{cutoff} meant cut-off wavelength. *T*₄₀₀ meant transmittance at 400 nm.

TABLE 3 Optical properties of the poly(benzimidazole imide) films.

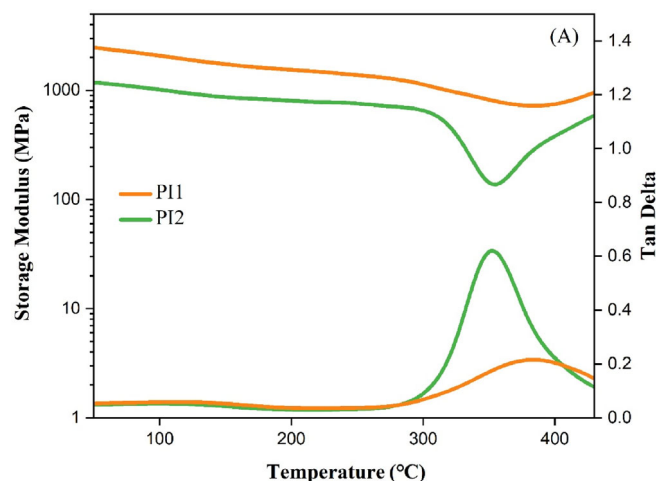


FIGURE 7 DMA curves of the poly(benzimidazole imide)s films.

(*T*_{d5%}) were measured under an atmosphere of nitrogen. The TGA curves of PI1 and PI2 were displayed in Figure 9, and the analysis data was summarized in Table 4. The introduction of CBDA provided alicyclic units for the PIs, which improved the backbone scission possibilities at high temperatures and the side groups (−CH₃ or −CF₃) decreased the chain packing. For these two reasons, the thermal properties had a decrease. However, the *T*_{d5%} for PI1 and PI2 could still reach 419 °C and 404 °C with the contribution of benzimidazole for the rod-like and rigid structures, respectively. The −CH₃ side groups in PI1 provided less free space volume than −CF₃ in PI2, resulting in higher *T*_{d5%} due to the stronger intermolecular interaction.

Figure 10 demonstrates a *T*₄₀₀-CTE diagram. The *T*₄₀₀ and CTE values in our previous studies were in the range of 10–81% and 22–52.2 ppm K^{−1}. Some of the films had good transparency (*T*₄₀₀ ≥ 80%), while the CTE value was extremely high (>40 ppm K^{−1}). The PIC had a low CTE value (22 ppm K^{−1}) but the transparency was not enough (*T*₄₀₀ = 44%).^{25,26,32} PI1 and PI2 in this study had better comprehensive properties (*T*₄₀₀ = 59% and CTE = 22 ppm K^{−1} in PI1 while

*T*₄₀₀ = 68% and CTE = 25 ppm K^{−1} in PI2). The reasons were as follows. First, the CBDA dianhydride and amide had stiff/linear structures good for the higher packing density, which led to lower CTE. Second, the −CH₃ or −CF₃ side groups could loosen the chain packing and hinder the formation of CTC, which was beneficial for transparency.

3.6 | Mechanical properties

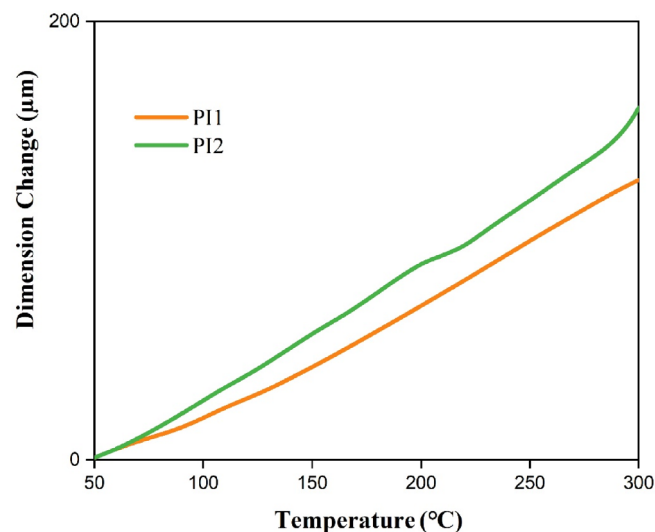
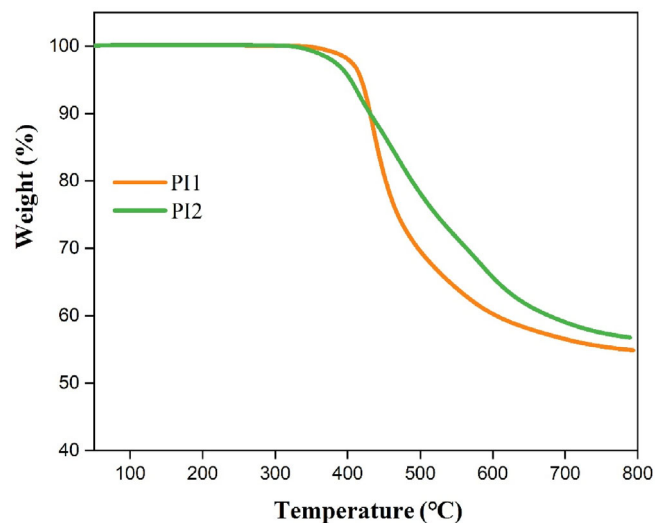
The mechanical properties are summarized in Figure 11 and Table 4. The initial modulus (*E*), tensile strength (σ), and elongation at break (ϵ) for PI1 and PI2 were 5.7 and 6.3 GPa, 120 and 138 MPa, 4.2 and 4.4%. The CBDA provided the PIs with more rigid/linear segments, which made the fracture mechanism change from ductile to brittle, thus the mechanical properties were restricted and resulted in lower elongation at break.⁴⁶ However, these PIs' tensile strength was more than 100 MPa and the initial modulus exceeded 2.0 GPa, which was enough for the AMOLED application.⁴⁷

3.7 | Water absorption

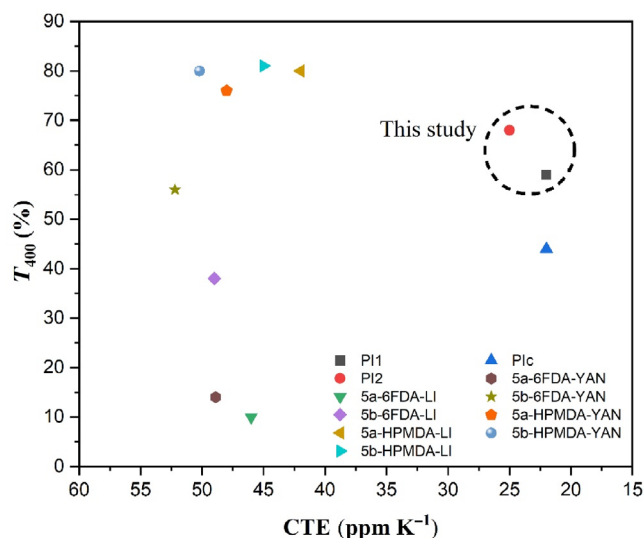
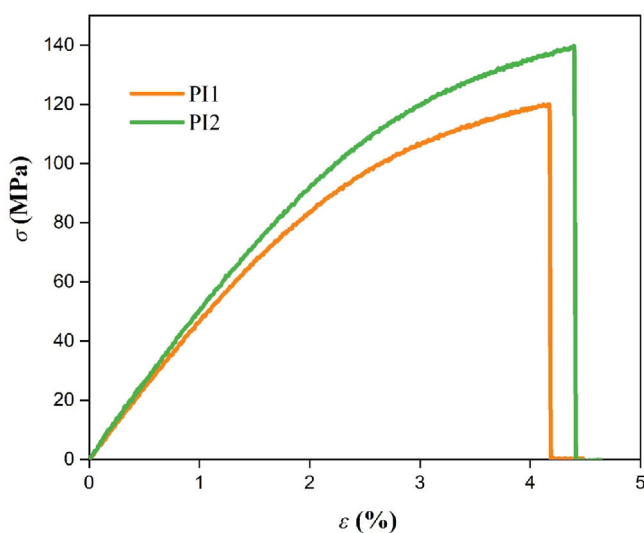
PIs were naturally absorbency due to the imide groups especially when there were benzimidazole and amide structures inside the chains. For example, the XOP2-360 (synthesized from 2-(4-aminophenyl)-1H-benzimidazol-2-amine (APBIA), 1,2,4,5-benzene tetracarboxylic anhydride (PMDA) and 4,4'-oxydipthalic anhydride (ODPA)) exhibited high *W*_A up to 5.1%.⁴⁸ The DPI (synthesized from 4,4'-diamino benzanilide [DABA] and 3,3',4,4'-Biphenyltetracarboxylic dianhydride [BPDA]) exhibited high *W*_A up to 3.6%.⁴⁹ The PMDA/DABA system also had high *W*_A up to 3.4%.⁵⁰ In this work, the *N*-substituent on benzimidazole is adverse to form a stable water network between its two kinds of nitrogen atoms so the *W*_A was mainly contributed by the bis-amide structure.⁵¹ The affinity of amide H-bonds with water molecules made PI1

TABLE 4 Basic properties of the poly(benzimidazole imide) films.

PIs	W_A (%)	T_g^a (°C)	$T_{d5\%}^b$ (°C)	CTE ^c (ppm K ⁻¹)	E (GPa)	σ (MPa)	ϵ (%)
PI1	2.9	386	419	22	5.7	120	4.2
PI2	2.0	351	404	25	6.3	138	4.4

^aGlass transition temperature measured by DMA at a heating rate of 5 °C min⁻¹ at 1 Hz.^b5% weight loss temperature measured by TGA in a nitrogen atmosphere at a heating rate of 10 °C min⁻¹.^cCoefficient of thermal expansion along the X–Y direction, measured in the range of 100–300 °C at a heating rate of 5 °C min⁻¹.**FIGURE 8** TMA curves of the poly(benzimidazole imide)s films.**FIGURE 9** TGA curves of the poly(benzimidazole imide)s films.

and PI2 absorb water more easily.^{52,53} The W_A of PI1 and PI2 were 2.9% and 2.0% respectively. The results were a bit lower than the systems mentioned above because of the bulky N-substituent and $-\text{CH}_3/-\text{CF}_3$

**FIGURE 10** Transparency-CTE diagram and polyimides containing benzimidazole.^{25,26,32}**FIGURE 11** Stress-strain curves of the poly(benzimidazole imide) films.

side groups. PI2 had a lower W_A for the low surface energy, small radius, and hydrophobicity of its fluorine atoms.^{27,48}

4 | CONCLUSION

Two new benzimidazole diamines (5a and 5b) were synthesized and polymerized with commercial dianhydride (CBDA) to obtain two kinds of PI films. The analysis indicated that the bis-amide groups and CBDA could make the CTE value reach a low level through their stiff/liner structures, as PI1 (CTE = 22 ppm K⁻¹) and PI2 (CTE = 25 ppm K⁻¹). The —CF₃ side group could make a bigger free space volume than —CH₃, so the PI2 has better optical properties (T_{400} = 68%, YI = 4.13). The T_g of PI1 and PI2 could reach 382 °C and 351 °C and the $T_{d5\%}$ were 415 °C and 404 °C. The side groups were good for manufacture as they loosened packing density resulting in good solubility in most organic solutions. The tensile strength was more than 100 MPa and the initial modulus was 5.7 and 6.3 GPa for PI1 and PI2, which was enough for optical application. The W_A of PI1 and PI2 were 2.9% and 2.0%, respectively. The results demonstrated that PI1 and PI2 would be promising candidates for colorless flexible substrates. In addition, a new synthesis and polymerization strategy was given to fabricate colorless polymer films with higher T_g and lower CTE.

ACKNOWLEDGMENTS

This work was supported by the Fundamental Research Funds for the Central Universities (2232023D-23).

ORCID

Gang Liu  <https://orcid.org/0009-0009-4077-5154>

REFERENCES

- [1] X. Pan, B. Wu, H. Gao, S. Chen, Y. Zhu, L. Zhou, H. Wu, S. Yu, *Adv. Mater.* **2022**, *34*, 2105299.
- [2] I. Gouzman, E. Grossman, R. Verker, N. Atar, A. Bolker, N. Eliaz, *Adv. Mater.* **2019**, *31*, 1807738.
- [3] H. Khaleel, H. Al-Rizzo, D. Rucker, *J. Disp. Technol.* **2012**, *8*, 91.
- [4] Y. Zhang, B. Liao, *Polym. Degrad. Stab.* **2023**, *215*, 110443.
- [5] H. Yoo, K. Park, M. Koo, S. Kim, S. Lee, S. Lee, K. Lee, *Proc. SPIE.* **2012**, *8268*, 82681Y.
- [6] Y. Liu, Q. Chen, P. Li, *Mater. Chem. Phys.* **2023**, *308*, 128247.
- [7] P. Tapaswi, C. Ha, *Macromol. Chem. Phys.* **2019**, *220*, 1800313.
- [8] L. Peng, W. Xie, S. Gong, F. Hu, *Polym. Polym. Compos.* **2023**, *31*, 1.
- [9] T. Matsumoto, *J. Photopolym. Sci. Technol.* **1999**, *12*, 231.
- [10] F. Bao, H. Lei, B. Zou, W. Peng, L. Qiu, F. Ye, Y. Song, F. Qi, X. Qiu, M. Huang, *Polymer* **2023**, *273*, 125883.
- [11] J. Chang, *Rev. Adv. Mater.* **2020**, *59*, 1.
- [12] Y. Xu, M. Zhang, Y. Pang, T. Zheng, C. Tian, Z. Wang, J. Yan, *Eur. Polym. J.* **2023**, *193*, 112099.
- [13] G. Liu, J. Zhang, Z. She, L. Peng, L. Qu, K. Wang, H. Tang, C. Yang, *Eng. Rep.* **2023**, *5*, e12617.
- [14] M. Yi, W. Huang, K. Choi, *J. Macromol. Sci. Part A: Pure Appl. Chem.* **1998**, *35*, 2009.
- [15] T. Matsumoto, T. Kurosaki, *React. Funct. Polym.* **1996**, *30*, 55.
- [16] K. Takizawa, J. Wakita, S. Azami, S. Ando, *Macromolecules* **2011**, *44*, 349.
- [17] Y. Liu, Y. Wang, D. Wu, *J. Appl. Polym. Sci.* **2022**, *139*, e52604.
- [18] X. Shi, S. Zhang, Q. Zhou, J. Li, B. Zhu, L. Xu, Q. Gao, *Tungsten* **2023**, *5*, 179.
- [19] M. Tsai, I. Tseng, S. Huang, C. Hsieh, *Int. J. Polym. Mater. Polym. Biomater.* **2014**, *63*, 48.
- [20] Y. Wang, W. Chen, *Compos. Sci. Technol.* **2010**, *70*, 769.
- [21] X. Jiang, K. Chen, C. Li, Y. Long, S. Liu, Z. Chi, J. Xu, Y. Zhang, *ACS Appl. Mater. Interfaces.* **2023**, *15*, 41793.
- [22] X. Zhi, G. Jiang, Y. Zhang, Y. Jia, L. Wu, Y. An, J. Liu, Y. Liu, *J. Appl. Polym. Sci.* **2022**, *139*, e51544.
- [23] Y. Zhang, Y. Zhou, Z. Wang, J. Yan, *J. Appl. Polym. Sci.* **2022**, *139*, e53082.
- [24] H. Zuo, G. Qian, H. Li, F. Gan, Y. Fang, X. Li, J. Dong, X. Zhao, Q. Zhang, *Polym. Chem.* **2022**, *13*, 2999.
- [25] D. Li, C. Wang, X. Yan, S. Ma, R. Lu, G. Qian, H. Zhou, *Polymer* **2022**, *254*, 125078.
- [26] X. Yan, F. Dai, Z. Ke, K. Yan, C. Chen, G. Qian, H. Li, *Eur. Polym. J.* **2022**, *164*, 110975.
- [27] H. Zuo, Y. Chen, G. Qian, F. Yao, H. Li, J. Dong, X. Zhao, Q. Zhang, *Eur. Polym. J.* **2022**, *173*, 111317.
- [28] Y. Wang, Y. Li, F. Li, J. Shen, J. Zhao, G. Tu, *Polym. Test.* **2023**, *129*, 108269.
- [29] H. Suzuki, T. Abe, K. Takaishi, M. Narita, F. Hamada, *J. Polym. Sci. Part A: Polym. Chem.* **2000**, *38*, 108.
- [30] M. Hasegawa, M. Horiuchi, Y. Wada, *High Perform. Polym.* **2007**, *19*, 175.
- [31] M. Hasegawa, *High Perform. Polym.* **2001**, *13*, S93.
- [32] D. Li, D. Li, Z. Ke, Q. Gu, K. Xu, C. Chen, G. Qian, G. Liu, *J. Polym. Sci.* **2023**, *61*, 818.
- [33] G. Qian, F. Dai, H. Chen, M. Wang, M. Hu, C. Chen, Y. Yu, *J. Polym. Sci.* **2021**, *59*, 510.
- [34] J. Miao, X. Hu, X. Wang, X. Meng, Z. Wang, J. Yan, *Polym. Chem.* **2020**, *11*, 6009.
- [35] J. Xing, G. Zhu, X. Fang, G. Chen, *J. Polym. Sci.* **2023**, *61*, 3276.
- [36] S. Lai, Y. Shi, W. Wu, B. Wei, C. Liu, L. Zhou, X. Huang, *Polym. Chem.* **2023**, *14*, 359.
- [37] G. Song, X. Zhang, D. Wang, X. Zhao, H. Zhou, C. Chen, G. Dang, *Polymer* **2014**, *55*, 3242.
- [38] L. Luo, J. Yao, X. Wang, K. Li, J. Huang, B. Li, H. Wang, Y. Feng, X. Liu, *Polymer* **2014**, *55*, 4258.
- [39] J. Tan, F. Xie, J. Huang, C. Zhao, X. Liu, H. Li, J. Yuan, Y. Liu, *React. Funct. Polym.* **2023**, *192*, 105703.
- [40] Y. Zhuang, J. Seong, Y. Do, W. Lee, M. Lee, M. Guiver, Y. Lee, *J. Membr. Sci.* **2016**, *504*, 55.
- [41] B. Zou, L. Qiu, H. Lei, J. Liu, W. Peng, H. Zhao, F. B. M. Huang, *Chin. J. Polym. Sci.* **2023**, *41*, 1599.
- [42] J. Ma, L. Yuan, S. Fan, L. Wang, B. Jia, H. Yang, S. Yang, *Eur. Polym. J.* **2023**, *192*, 112071.
- [43] D. Li, C. Wang, X. Yan, S. Ma, R. Lu, C. Chen, G. Qian, H. Zhou, *RSC Adv.* **2022**, *12*, 4234.
- [44] Z. Yang, H. Guo, C. Kang, L. Gao, *Polym. Chem.* **2021**, *12*, 5364.
- [45] M. Hasegawa, Y. Watanabe, S. Tsukuda, J. Ishii, *Polym. Int.* **2016**, *65*, 1063.
- [46] Y. Feng, L. B. Luo, J. Huang, K. Li, B. Li, H. Wang, X. Liu, *J. Appl. Polym. Sci.* **2016**, *133*, 1.

- [47] M. Lian, X. Lu, Q. Lu, *Macromolecules* **2018**, *51*, 10127.
- [48] K. Guo, J. Zhan, S. Qi, G. Tian, D. Wu, *Eur. Polym. J.* **2024**, *205*, 112723.
- [49] K. Zhang, Q. Yu, L. Zhu, S. Liu, Z. Chi, X. Chen, Y. Zhang, J. Xu, *Polymer* **2017**, *9*, 677.
- [50] M. Hasegawa, K. Koseki, *High Perform. Polym.* **2006**, *18*, 697.
- [51] D. Tomlin, A. Fratini, M. Hunsaker, W. Adams, *Polymer* **2000**, *41*, 9003.
- [52] T. Cao, X. Wang, R. Zhang, S. Chen, H. Qi, Y. Yao, F. Liu, *J. Polym. Sci.* **2023**, *61*, 1584.

- [53] Y. Liu, A. Tang, J. Tan, C. Chen, D. Wu, H. Zhang, *ACS Omega* **2021**, *6*, 4273.

How to cite this article: H. Zhang, F. Guo, K. Xu, M. Wang, C. Chen, G. Qian, G. Liu, Z. Deng, *J. Polym. Sci.* **2024**, *62*(12), 2716. <https://doi.org/10.1002/pol.20240048>